

# Evaluation of the cooling flow rate of the cooled steam turbine for a novel H<sub>2</sub>/O<sub>2</sub> cycle

## Original article

### Article history:

Submission date: 17 November 2023

Acceptance date: 7 March 2024

Publication date: 7 May 2024

This is the updated version of a paper originally presented at the Global Power and Propulsion Technical Conference, GPPS Hong Kong23, October 17–19, 2023.



### \*Correspondence:

XZ: zhxc@sjtu.edu.cn

### Peer review:

Single blind

### Copyright:

© 2024 Ma et al. © This is an open access article distributed under the Creative Commons Attribution Non Commercial No Derivatives License (CC BY-NC-ND 4.0). Unrestricted use, distribution, and reproduction of the original work are permitted for noncommercial purposes only, provided it is properly cited and its authors credited. No derivative of this work may be distributed.

### Keywords:

steam; hydrogen and oxygen combustion gas turbine; cooling efficiency; cooling flow requirement; cooling model

### Citation:

Ma B., Shi L., Li Y., Zhu X., and Du Z. (2024). Evaluation of the cooling flow rate of the cooled steam turbine for a novel H<sub>2</sub>/O<sub>2</sub> cycle. *Journal of the Global Power and Propulsion Society*. 8: 127–140. <https://doi.org/10.33737/jgpps/185742>

Bangyan Ma<sup>1</sup>, Lei Shi<sup>1</sup>, Yan Li<sup>2</sup>, Xiaocheng Zhu<sup>1\*</sup>, Zhaohui Du<sup>1</sup>

<sup>1</sup>Shanghai Jiao Tong University School of Mechanical Engineering, 800 Dongchuan RD. Minhang District, Shanghai 200240, China

<sup>2</sup>China United Gas Turbine Technology Co. Ltd, 6 Jiuxianqiao RD. Chaoyang District, Beijing 100016, China

## Abstract

In recent years, with the global low-carbon development, hydrogen as a clean fuel for the industry has attracted the interest of many research institutions all over the world. The potential of hydrogen energy in energy transformation has been paid attention to again. In the power generation industry, using hydrogen as gas turbine fuel is likely to play an important role in achieving carbon neutrality. At design stage, it is necessary to perform a preliminary evaluation of the performance of the novel hydrogen-fueled cycle with a few (or even without) experimental data. It is sure that secondary cooling systems have a significant impact on it. In this paper, a methodology is adopted for the cooling of hydrogen-fueled gas turbine. It is based on mass/energy balances and heat transfer correlations. The aim is to evaluate the turbine efficiency and cooling flow requirements of the novel hydrogen-fueled cycle. When both the working fluid and coolant are steam, the cooling flow rate is less. Preliminary results for the novel H<sub>2</sub>/O<sub>2</sub> cycle turbine show that part of the stages need to be cooled and the film cooling effectiveness is less.

## Introduction

Hydrogen, as a kind of clean energy, plays an important role in the power industry, especially when it is produced from renewable energy sources (solar and wind) or nuclear energy (Chiesa et al., 2005).

While hydrogen energy technology is becoming more mature, power generation systems based on hydrogen could be an important alternative to conventional power systems based on the combustion of fossil fuels (Milewski, 2015). Mixed hydrogen and pure hydrogen combustion in gas turbines is an important technological path to achieve carbon neutrality.

In response to the energy crisis of the last century, Westinghouse has worked to develop a hydrogen-fueled combustion turbine system designed to meet the goals set by the Japanese WET-NET Program (Bannister et al., 1999; Yang, 2006). Then, several proposed steam turbine thermodynamic cycle configurations, such as GRAZ (Desideri et al., 2001), TOSHIBA (Moritsuka and Koda, 1999), WESTINGHOUSE (Bannister et al., 1998), and MNRC (Miller et al., 2000) are presented. The efficiency of these cycles can achieve as high as 66.4%. The heating value of hydrogen is much higher than traditional fossil fuels. In addition, considering the fact that Hydrogen-Fueled Combustion Turbine Cycle almost eliminates CO<sub>2</sub> and NO<sub>x</sub> emissions, this solution could be viewed as an interesting alternative for future development compared to conventional power technologies.

It is sure that the turbine efficiency and cooling flow requirements have a considerable effect on the cycle efficiency (Scaccabarozzi et al., 2019). Therefore, in order to assess the performance of novel cycles, it is necessary to perform a preliminary evaluation of the turbine efficiency and cooling flow requirements based on a few (or even without) experimental data. Many models have been developed to estimate the cooling flow requirements and turbine efficiency for conventional gas turbines (working fluid is air). These models only depend on the geometric parameters of turbines and the behavior of the working fluid. Halls (1967), Holland and Thake, proposed the first semi-empirical cooling model. El-Masri (1986) proposed a cooling model, which treated the turbine as an expander whose walls continuously extract work. Consonni (1992) proposed the analytical model which considered the blade as a heat exchanger and calculated the distribution of the temperature of the coolant and the cooling efficiency. In the CO<sub>2</sub> cycle (working fluid is CO<sub>2</sub>), Jordal et al. (2004) used El-Masri's cooling model to evaluate the performance of the semi-closed O<sub>2</sub>/CO<sub>2</sub> cycle with CO<sub>2</sub> capture. Fiaschi et al. (2009) used the semi-empirical cooling model to evaluate the performance of an oxy-fuel combustion CO<sub>2</sub> power cycle. Scaccabarozzi et al. (2019) applied the analytical model to assess the performance of the cooled supercritical CO<sub>2</sub> turbine for the conceptual design.

In this paper, a methodology is proposed for the preliminary evaluation of the turbine efficiency and cooling flow requirements of a novel cycle based on the Hydrogen-Fueled Combustion Turbine Cycle. The thermodynamic analysis and optimization of the cycle are reported in the reference (Yu et al., 2023). Firstly, the novel cycle is shown in section 2. In section 3, the thermodynamic model used in this study is derived. Then, the results are discussed in section 4. At last, the conclusions are summarized in section 5.

## The novel H<sub>2</sub>/O<sub>2</sub> cycle

In this research, a novel H<sub>2</sub>/O<sub>2</sub> cycle is operated with pure hydrogen which is fired with pure oxygen (Yu et al., 2023). The stoichiometric oxygen-hydrogen ratio has been taken in this analysis, so the flue gas of this novel H<sub>2</sub>/O<sub>2</sub> cycle is pure steam.

It is a diffluent flow recompression novel H<sub>2</sub>/O<sub>2</sub> combined cycle which consists of the top cycle (red lines) and bottom cycle (blue lines). The top cycle is carried out by gas turbines and the bottom cycle is carried out by ultra-supercritical unit. Figure 1 presents a principal flow scheme of the novel cycle. The top cycle includes components 1–6. Hydrogen and oxygen enter the combustion chamber (component 1, CC) from outside. The working fluid exits the combustion chamber with a temperature of 1,500 °C and a pressure of around 3,800 kPa and then it is expanded to around 102 kPa (component 2, HTT). Cooling is done with a further recycled H<sub>2</sub>O stream. The energy of the turbine exhaust gas is used to heat the recycle stream in the recuperator (component 3, HRSG). After the recuperator, the cycle fluid is divided into two parts (red line and blue line). Part of the working fluid is compressed by the low-pressure compressor (component 4, C1). The working fluid is cooled by other steam streams in the intercooler (component 5). Finally, the working fluid is compressed again by the high-pressure compressor (component 6, C2).

The other part of working fluid separated (blue line) enters the bottom cycle and is expanded in the low-pressure steam turbine (component 7, LPT). Part of steam condenses into water during the expansion and enters the deaerator (component 10). The rest part of steam enters condenser 8 and pump 9, then mixes with the former in the deaerator (component 10). All of the condensates are pumped into the recuperator by the feed

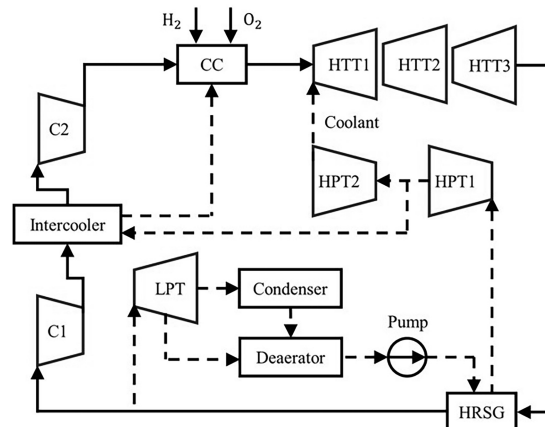


Figure 1. Scheme of the novel H<sub>2</sub>/O<sub>2</sub> cycle.

pump 11. The condensate is heated by the turbine exhaust gas in the recuperator (component 3, HRSG) and exits as high-pressure steam. This recycled steam is expanded in a high-pressure steam turbine (component 12, HPT1). Part of the exhaust steam enters the intercooler to cool the steam in the top cycle, and the other part of steam is expanded in a medium-pressure steam turbine (component 13, HPT2). The flue steam is used to cool the gas turbine.

This is an advanced form of the thermal cycle for future power generation systems. It can not only achieve the requirement of high efficiency (>70%), but also minimize carbon emissions, or even zero emissions. The working fluid in the top cycle and bottom cycle are both steam so they can mix while the working medium is still pure steam, which is more flexible than the conventional gas-steam combined cycle.

## Methodology

### The cooling model

In order to predict the cooling flow requirements and their effect on the turbine efficiency, a cooling model is presented. This model is a modification of the model proposed in the reference (Masci and Sciubba, 2018), henceforth referred to as the analytical model.

The blade channel is divided into many elementary layers along the span in the analytical model, as shown in Figure 2. The corresponding blade area of this elementary layer is,

$$dA_{b,g} = L_{b,g}dy \tag{1}$$

where,  $L_{b,g}$  is the gas side blade perimeter. In a similar way, there are also many layers in the internal cooling passages, as shown in Figure 3 and the corresponding area of layers in the internal cooling passages is,

$$dA_{b,c} = L_{b,c}dy \tag{2}$$

where,  $L_{b,c}$  is the gas side blade perimeter.

In each elementary layer, it is assumed that

1. The heat transfer process is steady.
2. The inlet gas temperature  $T_g$  remains unchanged along both the span and chord.
3. The heat transfer coefficient keeps constant along both the span and chord.
4. The conduction along the span is neglected.
5. The centrifugal effect of rotation on coolant is not considered.

According to the above assumptions, the heat transfer process is governed by following equations,

$$dq = HTC_g(T_g - T_{b,g}(y))dA_{b,g} \tag{3}$$

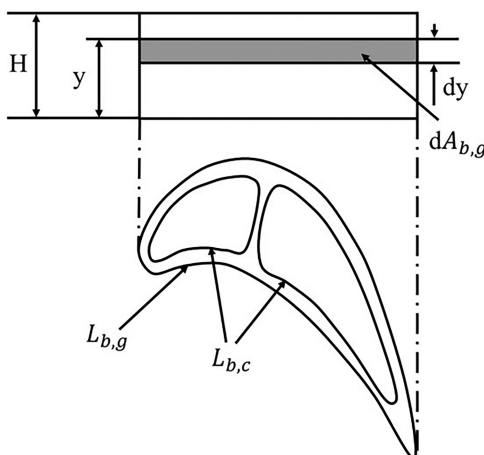


Figure 2. Elementary layer for heat transfer.

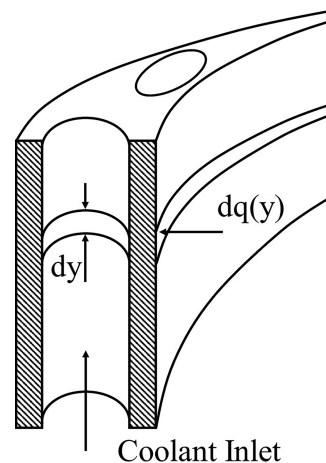


Figure 3. Elementary layer in internal cooling passages.

$$dq = \frac{\lambda_b}{t_b} (T_{b,g} - T_{b,c}(y)) dA_{b,g} \tag{4}$$

$$dq = \text{HTC}_c (T_{b,c} - T_c(y)) dA_{b,c} \tag{5}$$

Then the sum of three Equations 3–5 yields

$$dq = \left( \frac{1}{\text{HTC}_g dA_{b,g}} + \frac{t_b}{\lambda_b dA_{b,g}} + \frac{1}{\text{HTC}_c dA_{b,c}} \right)^{-1} (T_g - T_c(y)) \tag{6}$$

Let  $a_c = L_{b,c}/L_{b,g}$ , then

$$dq = \left( a_c \left( \frac{1}{\text{HTC}_g} + \frac{t_b}{\lambda_b} \right) + \frac{1}{\text{HTC}_c} \right)^{-1} (T_g - T_c(y)) dA_{b,c} \tag{7}$$

The overall heat transfer coefficient  $k$  is used to simplify the notation.

$$dq = k(T_g - T_c(y)) a_c L_{b,g} dy \tag{8}$$

where,  $k = \left( a_c \left( \frac{1}{\text{HTC}_g} + \frac{t_b}{\lambda_b} \right) + \frac{1}{\text{HTC}_c} \right)^{-1}$  and  $dA_{b,c} = L_{b,c} dy = a_c L_{b,g} dy$ .

In the internal cooling channel, the temperature of coolant increases due to heat transfer, which is governed by the conservation of energy,

$$dq = \dot{m}_c c_{pc} dT_c(y) \tag{9}$$

hence

$$\dot{m}_c c_{pc} dT_c(y) = k(T_g - T_c(y)) a_c L_{b,g} dy \tag{10}$$

The integration of this equation is then carried out along the span with the gas side perimeter  $L_{b,g}$ , the coolant mass flow rate  $\dot{m}_c$  and the coefficient  $a_c$  are all held unchanged. The boundary condition is  $T_c(0) = T_{c,in}$ .

Hence

$$T_c(y) = T_g - (T_g - T_{c,in}) e^{-\frac{k a_c L_{b,g} y}{\dot{m}_c c_{pc}}} \tag{11}$$

where,  $\bar{c}_{pc}$  is the span-wise mean value of  $c_{pc}$ .

$T_{b,g}(y)$  and  $T_{b,c}(y)$  can be obtained by solving Equations 3–5 with applying Equation 11. Obviously, for any value of  $y$ ,  $T_{b,g}(y) > T_{b,c}(y)$ , so the maximum blade temperature occurs at the tip of the gas side blade ( $y = H$ ),

$$T_{b,max} = T_g - \frac{a_c k}{\text{HTC}_g} (T_g - T_{c,in}) e^{-\left( \frac{k a_c L_{b,g} H}{\dot{m}_c c_{pc}} \right)} \tag{12}$$

which is limited by metallurgical considerations.

The heat transfer coefficient presented in Equation 12 can be calculated with Stanton number, namely,

$$\text{HTC} = \text{St} \cdot \rho U \cdot c_p \tag{13}$$

In the present paper, the external Stanton number is obtained from an empirical equation, as previously employed by Bergman et al. (2011),

$$St_g = 0.0296Re_g^{-0.2}Pr_g^{-(2/3)} \tag{14}$$

The cooling side heat transfer coefficient required by the analytical model can be determined by another empirical Equation 15 proposed by Colburn (Torbidoni and Horlock, 2005),

$$St_c = E_b \times 0.023Re_c^{-0.2}Pr_c^{-(2/3)} \tag{15}$$

where,  $E_b$  is a heat transfer enhancement factor associated with the presence of ribs and turbulators in the cooling passages. The value of  $E_b$  is between 2 and 6, although it is claimed that the value above 5 appears extremely difficult in practice (Consonni, 1992). Therefore, in general, the value of  $E_b$  is taken between 2 and 4 (Chowdhury et al., 2017). In the present paper,  $E_b = 3$ .

An iterative process is presented in this research aimed to predict the coolant consumption with a given maximum allowable blade material temperature (MABMT) shown in Figure 4.

1. Select any value as input for the initial coolant mass flow rate.
2. Calculate the maximum blade temperature.
3. If the calculated result is higher than the maximum allowable blade material temperatures, the coolant mass flow rate will be increased; otherwise, the coolant mass flow rate will be reduced.
4. Iterate until the difference between the maximum blade temperature and the maximum allowable blade material temperatures reaches the given precision.
5. Output the final coolant mass flow rate.

The convection cooling model depicted in the previous paragraph is now extended to the case where the coolant is ejected through slots or holes in blade surface. It decreases the temperature of the boundary layer at blade surface  $T_{aw}$  which can be obtained by introducing the film cooling effectiveness.

$$\eta_{ad} = \frac{T_g - T_{aw}}{T_g - T_{c,out}} \tag{16}$$

Then,  $T_{aw}$  is substituted for  $T_g$  in Equation 12, after considering the film cooling effect.

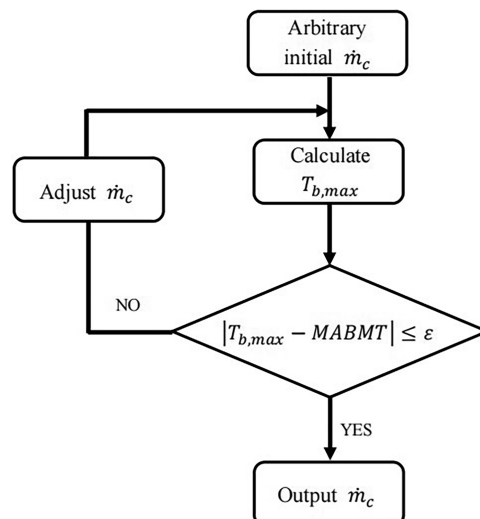


Figure 4. Iterative process of analytical model.

The film cooling effectiveness is obtained by using empirical Equation 17 proposed by Goldstein (1971).

$$\eta_{ad} = \frac{1.9Pr_g^{2/3}}{1 + 0.329(c_{pg}/c_{pc})\xi^{0.8}\beta} \tag{17}$$

where,

$$\beta = 1 + 1.5 \times 10^{-4} Re_f \frac{\mu_c W_g}{\mu_g W_c} \sin \alpha \tag{18}$$

$$\xi = \frac{x}{Ms} \left[ \frac{\mu_c}{\mu_g} Re_f \right]^{-0.25} \tag{19}$$

$Re_f$  is the Reynolds number based on the diameter of the film hole.

$$Re_f = \frac{\rho_c U_c s}{\mu_c} \tag{20}$$

$M$  is blowing rate

$$M = \frac{\rho_c U_c}{\rho_g U_g} \tag{21}$$

### Cooled expansion

In the present paper, it is assumed that the work is extracted from the expanding gas continuously rather than discretely, therefore, the turbine is considered as an expander. The evaluation of turbine loss and turbine work output can be obtained by following processes.

1. The expansion in the gas turbine is assumed to be a polytropic expansion process in each row (Figure 5, 1–2'), so the temperature at any point of expansion can be obtained by using:

$$\frac{T}{T_1} = \left( \frac{p}{p_1} \right)^{\eta_p(\gamma-1)/\gamma} \tag{22}$$

2. The losses occurring due to internal cooling leads to an isobaric temperature drop during the expansion in a particular row (Figure 5, 2'–2''). The enthalpy at point 2'' can be determined by applying the heat transfer

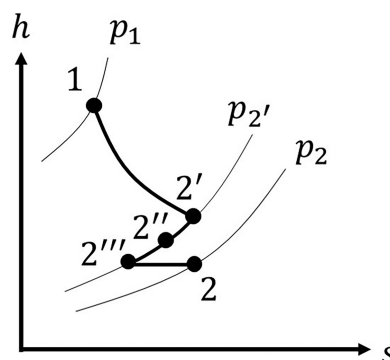


Figure 5. Expansion path in cooled turbine row.

equation:

$$\dot{m}_g(h_{g2'} - h_{g2''}) = \dot{m}_c(h_{c,out} - h_{c,in}) \quad (23)$$

3. The losses associated with the mixing of hot steam and coolant result in another isobaric temperature drop which can be calculated by solving the enthalpy balance equation (Figure 5,  $2'' - 2'''$ ):

$$\dot{m}_c h_{c,out} + \dot{m}_g h_{g2''} = (\dot{m}_c + \dot{m}_g) h_{g2'''} \quad (24)$$

4. The mixing pressure loss which is considered at the exit of the cooled row makes the state move from point  $2'''$  to point 2 isothermally. The pressure differences can be evaluated by equation (Kumar and Singh, 2010):

$$\frac{p_{2'} - p_2}{p_2} = 0.07 \times \frac{\dot{m}_c}{\dot{m}_g} \quad (25)$$

5. The work done by one row can be calculated by the following equation. The turbine work is the sum of work done by all rows cooled and uncooled.

$$w_{\text{row,cooled}} = h_1 - h_{2'} \quad (26)$$

6. The efficiency of turbine is defined as the ratio of the actual turbine specific work to the corresponding isentropic work.

## The properties of steam

The equation of state for steam can be obtained from IAPWS-IF97 which is adopted by the International Association for the Properties of Water and Steam (IAPWS) (Wagner et al., 2000). The dynamic viscosity of steam is calculated by using Sutherland's law (White and Majdalani, 2006):

$$\mu(T) = \mu_0 \left( \frac{T_0 + C}{T + C} \right) \left( \frac{T}{T_0} \right)^{3/2} \quad (27)$$

where,  $\mu_0 = 1.12 \times 10^{-5} \text{ Pa} \cdot \text{s}$ ,  $T_0 = 350 \text{ K}$ ,  $C = 1064 \text{ K}$ .

The specific heat of steam is known to be a function of temperature and pressure. However, in the present work specific heat of steam is assumed to be a function of temperature only, represented in the form of polynomials adopted from IAPWS-IF97 as follows:

$$c_p(T) = 416.504 \times (a + bT + cT^2 + dT^3) \quad (28)$$

Some main coefficients of the polynomial are shown in Table 1.

## Results and discussion

### The cooling flow requirements of a typical gas turbine

Compared with a conventional gas turbine, the cooling flow rate of a typical high-temperature turbine is estimated with steam as both working fluid and coolant. In this paper, GE-E<sup>3</sup> high-pressure turbine blade is selected and the detailed information can be found in the literature (Timko, 1984). This blade has 2 internal cooling passages where internal cooling can be implemented by flowing the coolant. Additionally, to prevent the hot main annulus gas of the turbine from overheating and damaging the blade, film cooling is applied to reduce the heat load.

Coolant consumption against gas temperature for steam and air as the working fluid is shown in Figure 6. The different solid line represents different coolant inlet temperature for air (500 K–900 K), similarly, the different dashed line represents different coolant inlet temperature for steam (500 K–900 K). The coolant consumption with air or steam as coolant increases with an increase in gas temperature almost linearly. For GE-E<sup>3</sup>, the



**Table 1.** The coefficients of the polynomial of the specific heat capacity for steam.

Coefficient	Value
<i>a</i>	3.878
<i>b</i>	$2.313 \times 10^{-4}$
<i>c</i>	$1.269 \times 10^{-6}$
<i>d</i>	$4.324 \times 10^{-10}$

inlet temperature is 2,012 K and coolant inlet temperature is 883 K at the design point. Hence, the corresponding coolant consumption is 6.31% which is close to the actual value of 6.3%. Therefore, the analytical model has been verified to be valid.

At a coolant inlet temperature of 500 K, the coolant consumption with steam as cooling medium is 24.73%, 22.89%, 21.19%, 19.54%, 17.89% and 16.25% less in comparison to the coolant consumption with air as cooling medium for gas temperature is 1,500 K, 1,600 K, 1,700 K, 1,800 K, 1,900 K and 2,000 K, respectively. It is reasonable that the specific heat capacity of steam is larger than that of air. However, at a coolant inlet temperature of 600 K, 700 K, 800 K and 900 K, the amount of cooling flow rate is more by applying cooling steam. The difference between performance of air cooling and steam cooling can be defined as:

$$\Delta = \frac{\dot{m}_{c,air} - \dot{m}_{c,steam}}{\dot{m}_{c,air}} \tag{29}$$

$\Delta$  presents the reduction degree of the cooling flow rate with the steam medium. Table 2 shows  $\Delta$  in detail. It is claimed that  $\Delta$  decreases with increase in gas temperature and first decreases and then increases with increase in coolant inlet temperature. In this paper, the maximum positive value of  $\Delta$  is 24.73% and the minimum negative value of  $\Delta$  is -22.31%.

### The performance of novel H2/O2 cycle turbine

The overall structure of turbines includes three cylinders which consist of high-pressure gas turbine, medium-pressure gas turbine and low-pressure gas turbine denoted by HTT1, HTT2 and HTT3 respectively. HTT1 and HTT2 are driven by high-pressure and low-pressure axial flow compressors respectively and HTT3 is a power turbine. Figure 7 shows the cross-sectional view of the turbines. Detailed information on the three turbines is

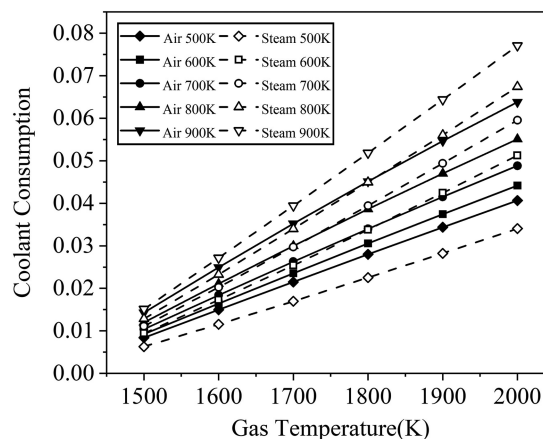


**Figure 6.** Effect of gas temperature and coolant inlet temperature on coolant consumption for steam and air as cooling medium.



Table 2. The difference between air cooling and steam cooling ( $\Delta$ ).

$\Delta$		Inlet temperature					
		1,500 K	1,600 K	1,700 K	1,800 K	1,900 K	2,000 K
Coolant inlet temperature	500 K	24.73%	22.89%	21.19%	19.54%	17.89%	16.25%
	600 K	-2.09%	-5.06%	-7.85%	-10.58%	-13.27%	-15.98%
	700 K	-6.85%	-10.04%	-13.07%	-16.04%	-18.98%	-21.93%
	800 K	-7.06%	-10.26%	-13.30%	-16.31%	-19.31%	-22.31%
	900 K	-5.75%	-8.85%	-11.84%	-14.82%	-17.79%	-20.78%

reported in Table 3. The coolant inlet temperature is low so that the coolant consumption can be reduced with steam cooling.

The H<sub>2</sub>/O<sub>2</sub> cycle studied in this paper is the optimized case presented in the reference (Yu et al., 2023). The resulting turbine operating conditions are:

- Turbine Inlet Mass Flow Rate: 334.98 kg/s
- Turbine Inlet Pressure: 3,800 kPa

The calculation is carried out for the uncooled case first and then for the cooled case to reveal the impact of cooling system on the performance and expansion. Both cases use the same inlet conditions.

For the cooled case, two kinds of maximum allowable blade material temperature distributions are applied. One is that the maximum allowable temperature remains unchanged at 1,250 K for all rows. However, materials with high melting points cost a lot, so in practice, it decreases along the expansion. Therefore, the other is that the maximum allowable temperature takes the value of 1,250 K, 1,200 K and 1,000 K for HTT1, HTT2 and HTT3 respectively.

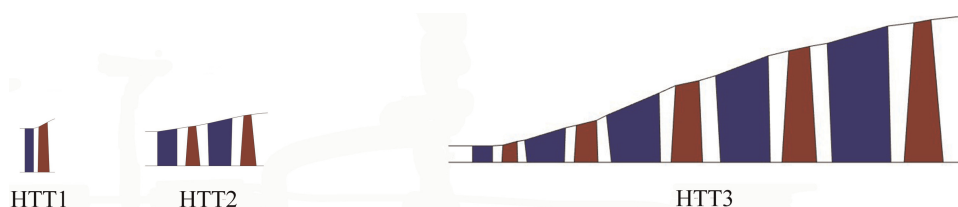


Figure 7. Turbine cross sectional view.

Table 3. Turbine analysis data.

Value		Turbine		
		HTT1	HTT2	HTT3
Parameter	Pressure ratio	1.31	1.76	16.24
	Coolant inlet temperature (K)	567.52	531.85	476.48
	Number of stages	1	2	5
	Polytropic efficiency	0.91	0.91	0.91

The results related to the novel H<sub>2</sub>/O<sub>2</sub> cycle turbine are represented in Table 4. It shows that all stages in HTT1 and HTT2 are cooled but in HTT3 only part of stages are cooled because the gas temperature is less than the allowable blade material temperature. The coolant consumption of any cooled row is less than 2%. The coolant mass flow rate and film cooling effectiveness decrease during the expansion in an individual turbine.

Note that the film cooling effectiveness values obtained here are lower than the ones reported in the literature for a conventional modern gas turbine, where it can arrive 0.3 (Uysal, 2020). The reason maybe is that the coolant consumption is less when the working fluid and coolant are both steam according to the previous section and less coolant is required for film cooling than conventional gas turbines, so the film cooling effectiveness is less.

The comparison of performances is reported in Tables 5 and 6. For the case with different maximum allowable blade material temperatures, the isentropic efficiency with consideration of the cooling effect of three turbines is 1.29%, 1.72% and 3.39% less than those without consideration of the cooling effect, respectively. The losses caused by cooling system increase with the increase of coolant consumption.

The performance of HTT1 and HTT2 are almost the same for the cases with different and uniform maximum allowable blade material temperatures. For the last turbine with uniform maximum allowable blade material temperature, since 6 rows are not cooled, the isentropic efficiency and specific work are closer to the uncooled case.

Steam pressure against temperature is shown in Figure 8. The two p-T curves on the left (solid line) represent the cooled turbine while the p-T curve on the right (dashed line) represents the uncooled turbine. It is illustrated

Table 4. Film cooling effectiveness and coolant consumption of each row.

Turbine	Row	Maximum allowable temperature (K)	$\eta_{ad}$	$\dot{m}_c/\dot{m}_g$	Maximum allowable temperature (K)	$\eta_{ad}$	$\dot{m}_c/\dot{m}_g$
HTT1	Stator 1	1,250	0.220	1.69%	1,250	0.220	1.69%
	Rotor 2		0.195	1.61%		0.195	1.61%
HTT2	Stator 1	1,200	0.242	1.60%	1,250	0.211	1.35%
	Rotor 2		0.190	1.51%		0.164	1.27%
	Stator 3		0.192	1.48%		0.162	1.21%
	Rotor 4		0.145	1.27%		0.122	1.05%
HTT3	Stator 1	1,000	0.272	1.91%	1,250	0.113	0.63%
	Rotor 2		0.229	1.80%		0.079	0.52%
	Stator 3		0.226	1.82%		0.051	0.31%
	Rotor 4		0.159	1.32%		0.015	0.10%
	Stator 5		0.139	1.09%		0.000	0.00%
	Rotor 6		0.094	0.81%		0.000	0.00%
	Stator 7		0.057	0.44%		0.000	0.00%
	Rotor 8		0.010	0.06%		0.000	0.00%
	Stator 9		0.000	0.00%		0.000	0.00%
	Rotor 10		0.000	0.00%		0.000	0.00%

Table 5. The isentropic efficiency for the uncooled and the cooled cases.

Isentropic efficiency	Turbine		
	HTT1	HTT2	HTT3
Uncooled	91.20%	91.64%	93.46%
Cooled (different maximum allowable temperature)	89.91%	89.92%	90.07%
Cooled (uniform maximum allowable temperature)	89.91%	90.17%	92.86%

that the temperature of the main stream of cooled turbine with uniform maximum allowable blade material temperature is a little higher than that of cooled turbine with different maximum allowable blade material temperatures, and they are both lower than that of uncooled case.

### Conclusions

In this paper, the analytical model is used to compare the cooling performance with the different cooling mediums (air and steam). A methodology for the preliminary performance estimation without experimental data of the novel H<sub>2</sub>/O<sub>2</sub> cycle turbine is presented. All stages in HTT1 and HTT2 are cooled but in HTT3 only part of stages is cooled to protect the blade from hot gas.

Table 6. The actual specific work for the uncooled and the cooled cases.

Specific work (kJ/kg)	Turbine		
	HTT1	HTT2	HTT3
Uncooled	174.98	474.14	1,286.98
Cooled (different maximum allowable temperature)	172.51	465.24	1,240.32
Cooled (uniform maximum allowable temperature)	172.51	466.54	1,278.76

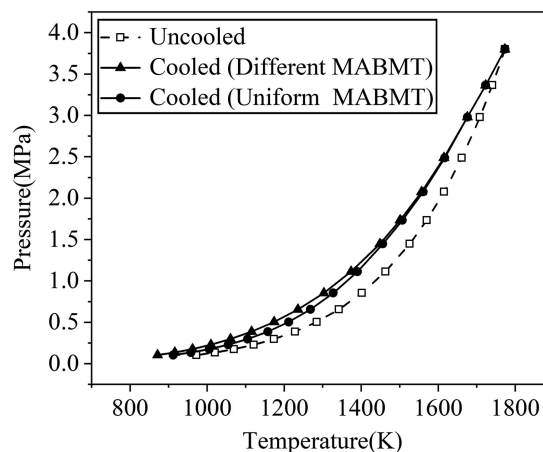


Figure 8. Pressure – temperature expansion diagram for the cooled and uncooled cases.

Main conclusions are summarized as follows:

1. The result obtained by applying analytical model on GE-E<sup>3</sup> high-pressure turbine agrees well with the design data, which demonstrates that the model is valid.
2. The coolant consumption with steam as cooling medium is less in comparison to the coolant consumption with air as cooling medium because the specific heat capacity of steam is larger than that of air at low coolant inlet temperature. More coolants are required by applying steam cooling at high coolant inlet temperature. The difference between performance of air cooling and steam cooling decreases with increase in gas temperature and first decreases and then increases with increase in coolant inlet temperature.
3. The amount of coolant used for film cooling with steam as cooling medium is less than that with air as cooling medium and the film cooling effectiveness values obtained here are lower than the ones reported in the literature for a conventional gas turbine. The penalty due to applying cooling system is significant. Like specific work, the isentropic efficiency with consideration of the cooling effect of HTT1, HTT2 and HTT3 is 1.29%, 1.72% and 3.39% less than those without consideration of the cooling effect, respectively.

## Nomenclature

---

### Latin symbols

$A$	area
$a_c$	$= L_{b,c}/L_{b,g}$
$c_p$	specific heat at constant pressure
$E_b$	parameter that considers increased surface of cooling channels due to turbulators
$H$	blade height
$h$	specific enthalpy
$k$	overall heat transfer coefficient
$L$	perimeter
$M$	blowing rate
$\dot{m}$	mass flow rate
Pr	Prandtl number
$p$	pressure
$q$	heat flux
Re	Reynolds number
$Re_f$	Reynolds number based on diameter of film hole
St	Stanton number
$s$	diameter of film hole
$T$	temperature
$U$	velocity
$W$	molecular weight
$w$	specific work
$x$	distance from point of injection
$y$	radial [span-wise] coordinate

### Greek symbols

$\alpha$	angle of injection for film cooling
$\gamma$	adiabatic index
$\Delta$	the reduction degree of the cooling flow rate with the steam medium
$\varepsilon$	a given precision
$\eta_{ad}$	film cooling effectiveness
$\eta_p$	polytropic efficiency
$\lambda$	conductivity
$\mu$	dynamic viscosity
$\rho$	density

## Subscripts

air	air
$aw$	the boundary layer at blade surface
$b$	blade
$c$	coolant, cooling side
cooled	cooled row
$g$	gas, gas side
$in$	inlet
max	maximum
$out$	outlet
row	row
steam	steam
1, 2', 2'', 2''', 2	different points during the polytropic expansion process

## Abbreviations

C	compressor
CC	combustion chamber
HPT	high-pressure steam turbine
HTC	heat transfer coefficient
HTT	gas turbine
LPT	low-pressure steam turbine
MABMT	maximum allowable blade material temperature

## Funding sources

Science Center for Gas Turbine Project (P2021-A-I-003-002) of the China.

## Competing interests

Bangyan Ma declares that he has no conflict of interest. Lei Shi declares that he has no conflict of interest. Yan Li declares that she has no conflict of interest. Xiaocheng Zhu declares that he has no conflict of interest. Zhaohui Du declares that he has no conflict of interest.

## References

- Bannister R. L., Newby R. A., and Yang W. C. (1998). Development of a hydrogen-fueled combustion turbine cycle for power generation. *Journal of Engineering for Gas Turbines and Power*. 120(2): 276–283. <https://doi.org/10.1115/1.2818116>.
- Bannister R. L., Newby R. A., and Yang W. C. (1999). Final report on the development of a hydrogen-fueled combustion turbine cycle for power generation. *Journal of Engineering for Gas Turbines and Power*. 121(1): 38–45. <https://doi.org/10.1115/1.2816310>.
- Bergman T. L., Lavine A. S., Incropera F. P., and Dewitt D. P. (2011). *Fundamentals of Heat and Mass Transfer*. 7th ed. USA: John Wiley & Sons, Hoboken.
- Chiesa P., Lozza G., and Mazzocchi L. (2005). Using hydrogen as gas turbine fuel. *Journal of Engineering for Gas Turbines and Power*. 127(1): 73–80. <https://doi.org/10.1115/1.1787513>.
- Chowdhury N. H., Zirakzadeh H., and Han J. C. (2017). A predictive model for preliminary gas turbine blade cooling analysis. *Journal of Turbomachinery*. 139(9): 091010. <https://doi.org/10.1115/1.4036302>.
- Consonni S. (1992). *Performance Prediction of Gas/Steam Cycles for Power Generation*. (Volumes I and II). Ph.D. Princeton University.
- Desideri U., Ercolani P., and Yan J. (2001). Thermodynamic analysis of hydrogen combustion turbine cycles. In Proc. of the ASME Turbo Expo.
- El-Masri M. A. (1986). On thermodynamics of gas-turbine cycles: part 2—a model for expansion in cooled turbines. *Journal of Engineering for Gas Turbines and Power*. 108(1): 151–159. <https://doi.org/10.1115/1.3239862>.
- Fiaschi D., Manfreda G., Mathieu P., and Tempesti D. (2009). Performance of an oxy-fuel combustion CO<sub>2</sub> power cycle including blade cooling. *Energy*. 34(12): 2240–2247. <https://doi.org/10.1016/j.energy.2008.12.013>.
- Goldstein R. A. (1971). Film cooling. *Advances in Heat Transfer*. 331–337. [https://doi.org/10.1016/S0065-2717\(08\)70020-0](https://doi.org/10.1016/S0065-2717(08)70020-0).
- Halls G. A. (1967). Air cooling of turbine blades and vanes: an account of the history and development of gas turbine cooling. *Aircraft Engineering and Aerospace Technology*. 39(8): 4–14. <https://doi.org/10.1108/eb034284>.
- Jordal K., Bolland O., and Klang A. K. (2004). Aspects of cooled gas turbine modelling for the semi-closed O<sub>2</sub>/CO<sub>2</sub> Cycle with CO<sub>2</sub> capture. *Journal of Engineering for Gas Turbines and Power*. 126(3): 507–515. <https://doi.org/10.1115/1.1762908>.
- Kumar S. and Singh O. (2010). Thermodynamic performance evaluation of gas turbine cycle with transpiration cooling of blades using air vis-à-vis steam. *Proceedings of the Institution of Mechanical Engineers, Part A: Journal of Power and Energy*. 224(8): 1039–1047. <https://doi.org/10.1243/09576509JPE964>.

- Masci R. and Sciubba E. (2018). A lumped thermodynamic model of gas turbine blade cooling: prediction of first-stage blades temperature and cooling flow rates. *Journal of Energy Resources Technology*. 140(2): 020901. <https://doi.org/10.1115/1.4038462>.
- Milewski J. (2015). Hydrogen utilization by steam turbine cycles. *Journal of Power Technologies*. 95(4): 258–264.
- Miller A., Milewski J., and Kiryk S. (2000). Remarks on hydrogen fuelled combustion turbine cycle. In Proc. of the Second International Scientific Symposium Compower. 239–248.
- Moritsuka H. and Koda E. (1999). Hydrogen-oxygen fired integrated turbine system-comparison on MORITS and GRAZ. In Proc. of IGTC 99 Kobe. 401–404.
- Scaccabarozzi R., Martelli E., Gatti M., Chiesa P., Pini M., et al. (2019). Conceptual thermo-fluid dynamic design of the cooled supercritical CO<sub>2</sub> turbine for the allam cycle. In Proc. of 11th International Conference on Applied Energy.
- Timko L. P. (1984). Energy Efficient Engine High Pressure Turbine Component Test Performance Report (No. NASA-CR-168289).
- Torbidoni L. and Horlock J. H. (2005). A new method to calculate the coolant requirements of a high-temperature gas turbine blade. *Journal of Turbomachinery*. 127(1): 191–199. <https://doi.org/10.1115/1.1811100>.
- Uysal S. C. (2020). Analysis of gas turbine cooling technologies for higher natural gas combined cycle efficiency. In Proc. of AIAA Propulsion and Energy 2020 Forum. 3697.
- Wagner W., Cooper J. R., Dittmann A., Kijima J., Kretzschmar H., et al. (2000). The IAPWS industrial formulation 1997 for the thermodynamic properties of water and steam. *Journal of Engineering for Gas Turbines and Power*. 122(1): 150–184. <https://doi.org/10.1115/1.483186>.
- White F. M. and Majdalani J. (2006). *Viscous Fluid Flow*. 3rd ed. New York: McGraw-Hill.
- Yang W. C. (2006). Hydrogen-fueled power systems. In: *The Gas Turbine Handbook*, edited by Dennis R. Morgantown: U.S. Department of Energy, 107–115.
- Yu S. D., Hu B., Li X. S., Ren X. D., Li X., and Gu C.W. (2023). Thermodynamic and economic analysis of a revised Graz cycle using pure oxygen and hydrogen fuel. *International Journal of Hydrogen Energy*. 48(98): 38907–38921. <https://doi.org/10.1016/j.ijhydene.2023.06.157>.